

Digital electro spray for controlled deposition

Weiwei Deng,¹ C. Mike Waits,² and Alessandro Gomez^{1,a)}

¹*Department of Mechanical Engineering, Yale University, 9 Hillhouse Ave., New Haven, Connecticut 06520, USA*

²*Army Research Laboratory, 2800 Powder Mill Rd., Adelphi, Maryland 20783, USA*

(Received 26 August 2009; accepted 7 February 2010; published online 30 March 2010)

Many novel functional structures are now fabricated by controlled deposition as a maskless, bottom-up fabrication technique. These applications require rapid and precise deposition of minute amounts of solutions/suspensions or their ultimate particle products in predefined patterns. The electro spray is a promising alternative to the commonly used inkjet printing because it can easily handle highly viscous liquid, avoid high shear rates, and has low risk of clogging. We demonstrate a proof-of-concept *digital* electro spray. This system consists of a 61-nozzle array microfabricated in silicon and a 61-element digital extractor fabricated using flexible polyimide substrates. “Digital” refers to the state of each electro spray source that can be tuned either on or off independently and responsively. We showed a resolution of 675 μm and a response frequency up to 100 Hz. With similar design and industry standard fabrication procedures, it is feasible to scale up the system to O(1000) sources with spatial resolution better than 250 μm and a O(kHz) response frequency. The latter is controlled by the viscous damping time. © 2010 American Institute of Physics.

[doi:[10.1063/1.3340907](https://doi.org/10.1063/1.3340907)]

I. INTRODUCTION

Controlled deposition has drawn enormous interest recently as a maskless, bottom-up fabrication technique for many novel functional structures such as all-polymer transistor circuits,¹ color polymer light emissive diode,² transparent electrode for solar cells,³ functional ceramics,⁴ and drugs in oral dosage form.⁵ These applications require rapid and precise deposition of either picoliters of solutions/suspensions or their final particle product in predefined patterns. Currently the dominant deposition technique is inkjet printing (IJP), which has been successfully applied to dispense inorganic particles, polymers,⁶ and live cells.⁷ The IJP print head uses a short pressure pulse generated either thermally or piezoelectrically to expel one or more ~ 100 pl liquid droplets out of a nozzle whose typical orifice dimension is 30–60 μm . The working principle of IJP may impose several restrictions on the type of suspension and solution it can handle. For example, the instantaneous pressure pulse introduces high shear rate of $\sim 10^5/\text{s}$,⁶ which may cause potential damage of the labile content of the suspension, such as live cells. The IJP also limits the liquid viscosity to 20 cP,⁶ which is below the viscosity of many polymer solutions of medium to high concentrations.

These IJP limitations can be easily overcome by the electro spray (ES) because of its entirely different atomization mechanism that relies solely on electric charging. A typical ES system can be implemented by feeding a liquid with sufficient electric conductivity through a capillary that is

charged at high potentials relative to a nearby ground electrode. Among many of the modes that ES can be operated in,⁸ the most remarkable one is the *cone-jet* mode. In this mode, the liquid meniscus takes a conical shape⁹ with a fine jet issuing from the cone tip. Clogging is generally not an issue for ES even with suspensions of high particulate concentrations because the ES capillary bore is typically two orders of magnitudes larger than the jet/droplet diameter. For the same reason, the ES can also easily handle high viscosity solutions without causing a substantial pressure drop. Additionally, the shear rate in an ES is generally more modest than in IJP. Another key feature of the ES is the quasimonodispersity of the droplets. The ES capability of producing monodisperse droplets with relative ease is unmatched by any other droplet generation scheme, especially in the sub-micron range. Since, when the deposition device is mounted on a precision translational stage, as is typically the case in IJP, the resolution is primarily determined by the droplet size, it is reasonable to expect that ES controlled deposition might exhibit better spatial resolution as compared to IJP. A line width of 100 nm and pattern resolution of ~ 10 μm using a single ES source have been demonstrated. To avoid spray expansion due to Coulombic repulsion among charged droplets, a few approaches have been implemented, including bringing the substrate very close (less than 100 μm) to the ES source before the spray expands,¹⁰ refocusing the spray electrostatically using a sharp grounded electrode below the substrate,¹¹ or predefining the pattern on a semiconducting or nonconducting substrate via contact charging.¹²

Cone-jet ES dispersion works only with electrically conductive fluids, which may pose some constraints in controlled deposition applications. But the major ES drawback is the low flow rate at which the cone-jet can be established.

^{a)}Author to whom correspondence should be addressed. Electronic mail: alessandro.gomez@yale.edu. Telephone: 203-432-4384. Fax: 203-432-7654.

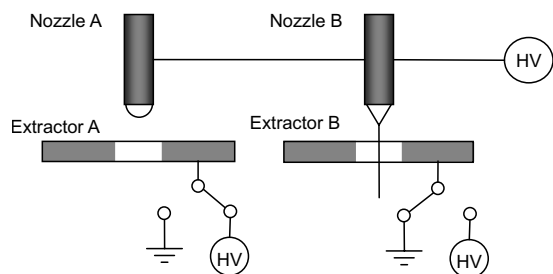


FIG. 1. Morphology of the liquid meniscus subject to different electric fields.

This drawback has been addressed through recent progress in multiplexing ES (MES) techniques, demonstrating the simultaneous operation of hundreds of ES sources¹³ and a remarkable packing density exceeding 10^4 sources/cm².¹³ The dispersion of the total flow rate among a large number of sources enables the low flow rate required for cone-jet operation to be maintained. However, the large number of ES sources in these MES devices must operate in unison, which may limit the flexibility of the device. Instead, independent control of the on/off behavior of each individual ES source is extremely appealing because of its potential in numerous applications, including controlled depositions.

In this contribution, we demonstrate a proof-of-concept *digital* ES, where “digital” refers to an ES source having only *on/off* states, just like a flip/flop circuit. We built this system using a microfabricated silicon nozzle array and low-cost flexible circuits to control each individual ES source.

II. EXPERIMENTAL APPROACH

A. Design overview

The working principle of the digital ES is based on the fact that a liquid meniscus suspended on the tip of a capillary may take different shapes depending on the applied electric field, which can be effectively localized by a nozzle-extractor configuration. Figure 1 shows the schematic of two identical nozzles charged at the same high potential. Nozzle A faces Extractor A, which is charged at the same high potential; therefore, no electric field or electric stress appears on the liquid meniscus surface. As a result, the meniscus takes a semispherical shape because of surface tension. In other words, the ES is turned off. The reason why no mass is ejected under these conditions is that the capillary effect is sufficient to compensate for the modest hydrostatic head in the liquid supply. On the other hand, an intense electric field is applied to the meniscus on Nozzle B since Extractor B is grounded. The balance between the electric stress and the surface tension results in a conical shape from which a jet is issued and the ES is turned on. The concept schematized in Fig. 1 suggests that it is possible to control the on/off state of either a single or a group of nozzles charged at a common high voltage, as long as the electric field is locally differentiated by electrically separating each corresponding extractor from each other or by doing so for groups of extractors, depending on the desired spatial resolution of the deposition pattern.

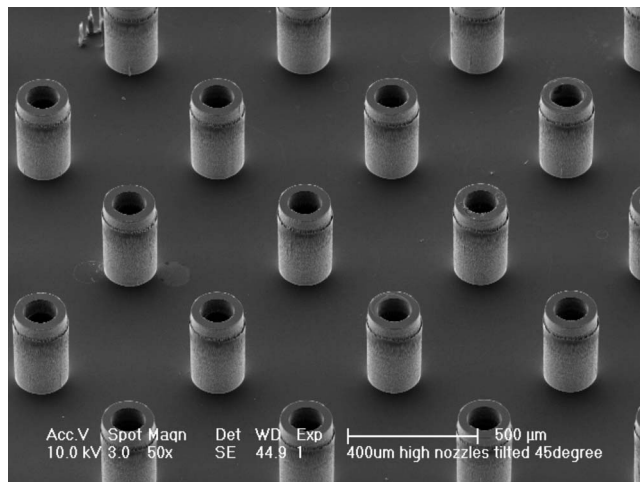


FIG. 2. The microfabricated nozzle array.

B. Microfabricated nozzle array

The centerpiece of the digital ES system is an array of closely packed nozzles. The device, shown in Fig. 2, was microfabricated using a series of photolithography and deep reactive ion etch steps in silicon wafers. The array has a packing density of 253 sources/cm². Uniform nozzles with an outer diameter of 210 μm , inner diameter of 120 μm , interspaced at 675 μm , and protruding 450 μm were patterned. The detailed fabrication, testing, and fundamentals of the nozzle array and assembly with a liquid reservoir were documented in Refs. 13–15. The working liquid is pure ethanol with an electrical conductivity measured at 1.3×10^{-5} S/m. The liquid was pumped continuously into the reservoir by a syringe pump with different syringe sizes to ensure that the plunger would be displaced at a reproducible and accurate speed.

C. Digital extractor

The key element that distinguishes the digital ES from a regular MES device is the digital extractor, which requires a complex wiring scheme to connect each extractor to the on/off control potentials. We fabricated the digital extractor prototype using a multiple-layer flexible circuits technique (Tech-Etch). The digital extractor consists of three etched copper conducting layers and two additional polyimide insulation layers that separate the copper layers. Figure 3 shows a computer-aided design (CAD) drawing of the three copper layers of the digital extractor with 61 conducting rings. The top copper layer addresses 22 extractor holes, the middle copper layer addresses the remaining 39 extractor holes, and the bottom layer faces the nozzle array. The bottom layer minimizes potential perturbations of the contact wires in the middle and top layers, which might have caused undesired ES firing, since it presents only extractor rings with no wires. The distance between two neighboring extractor rings is identical to the internozzle distance (675 μm).

To demonstrate the proof-of-concept system, we built a control panel with an array of 61 switches to control the digital extractor (Fig. 4). Each switch controls one extractor in the flexible circuits.

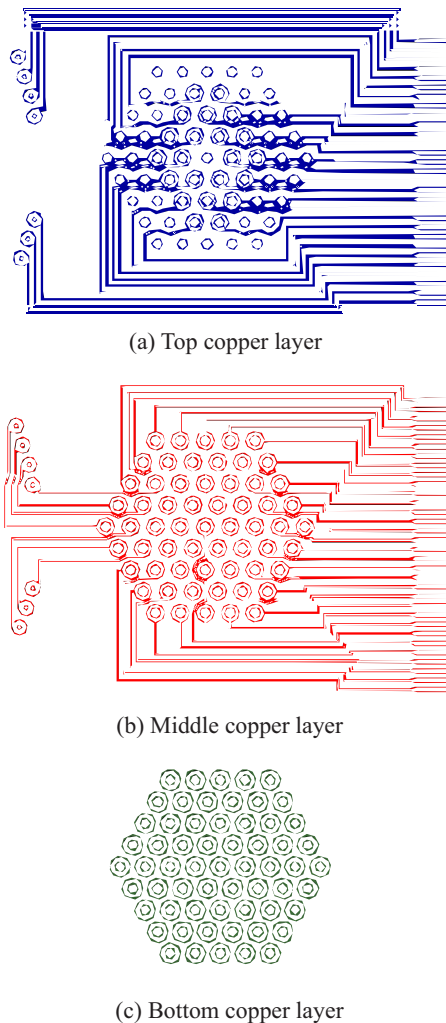


FIG. 3. (Color online) CAD drawing of a three-layer flexible circuit design of a 61 digital extractor system.

D. Electrode arrangement

The digital ES system consists of 61 sets of nozzle, extractor, and switch. Three sets are shown schematically in Fig. 5. The nozzle array, which was mounted on a liquid reservoir, was charged at high potential V_1 . One end of the digital extractor electrode was aligned and positioned $300\ \mu\text{m}$ below the tip of the nozzles with a polyimide spacer/insulator. The other end of the digital extractor was connected to the control panel that was shown in Fig. 4, which routed the individual extractor to ground (ES on) or V_2 (ES off). Ideally, V_2 should be the same as V_1 so no electric field will appear as V_2 is selected. However, the digital extractor can only withstand a voltage difference up to $750\ \text{V}$ between two neighboring extractors because of the risk of electric arcing for the designed pitch of $675\ \mu\text{m}$. Therefore, V_2 is limited to $750\ \text{V}$. To suppress further any accidental electric arcing, we connected a $1\ \text{G}\Omega$ power resistor to the potential sources V_2 and the ground. A driving field¹³ that prevents the droplets from flying back to the extractor is established by charging a flat metal collector electrode $\sim 5\ \text{mm}$ away from the extractor at V_3 . The flat metal

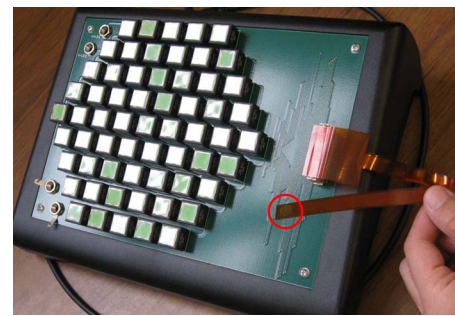


FIG. 4. (Color online) Control panel for the digital extractor. The end of the brown polyimide ribbon (highlighted in the circle) is the functioning part of the digital extractor.

collector acts as the substrate that the ES solution will be deposited on. A typical set of electric potentials applied are $V_1 = 1200\ \text{V}$, $V_2 = 750\ \text{V}$, and $V_3 = -5000\ \text{V}$.

E. Visualization and high speed photography

Visual observation of the ESs was made possible by a laser beam, which was first expanded and then focused by a $300\ \text{mm}$ cylindrical lens into a laser sheet. The laser sheet could be either parallel or perpendicular to the distributor surface. For the parallel orientation, the scattering of charged droplets in each spray resulted in the visualization of individual spray cross sections appearing as small circular spots, while the perpendicular orientation allowed for the visualization of spray plumes.

To measure the time needed for the transient process going from a hemisphere to a stable cone-jet, we recorded the ES transient process of a single microfabricated silicon nozzle taken from a large nozzle array using a high speed camera. The working liquid was ethanol pumped at the flow rate of $0.4\ \text{cc/h}$, a typical value for the average flow rate per nozzle in the digital ES. A high speed camera (Phantom v7.3), capable of acquiring pictures at up to $25\ 000\ \text{fps}$, was coupled with a microscope having a magnification of $20\times$. The on/off control of the ES was achieved by a switch allowing for a fast potential rise ($\sim 5\ \mu\text{s}$).

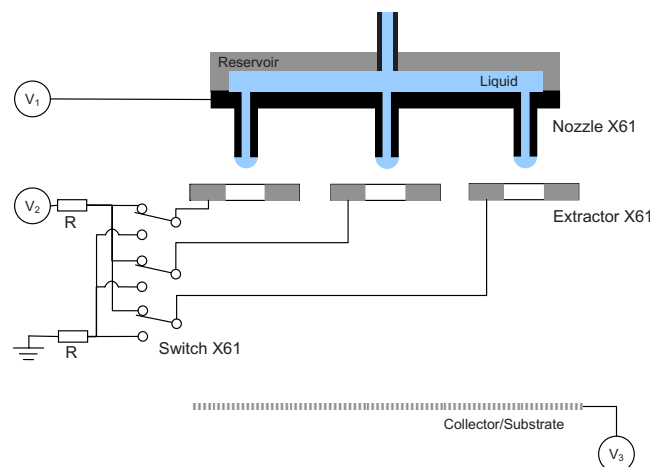
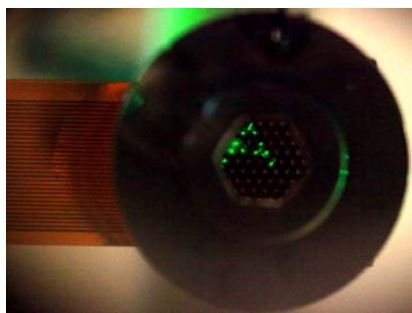
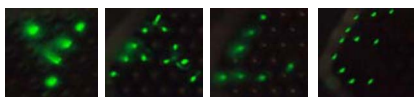


FIG. 5. (Color online) Electrode arrangement of the digital ES. (Packing density: $253\ \text{sources/cm}^2$; number of nozzles: 61; nozzle outer diameter: $210\ \mu\text{m}$; inner diameter: $120\ \mu\text{m}$; distance between two neighboring nozzles: $675\ \mu\text{m}$; nozzle protrusion: $450\ \mu\text{m}$.)



(a) Collector with a hexagon hole for picture taking



(b) The “YALE” pattern generated by the digital electrospay

FIG. 6. (Color online) Digital ES “writing.”

III. RESULTS AND DISCUSSIONS

A. Digital MES operation

The digital ES performed as expected: each ES responded to the on/off state set from the control panel. In other words, each liquid meniscus changes morphology accordingly to the change in the local electric field. Moreover, the on/off response of each ES source is highly repeatable. With respect to long-term operation, it is as stable as for the regular MES systems, so long as the driving field is sufficiently intense to avoid droplet fly back to the extractor.¹³ Most importantly, two neighboring ES sources can be set at different states, which suggest the extractors indeed effectively localize the electric field. This fact allows us to “display” a predefined pattern. For example, in Fig. 6, we show “YALE” displayed by the same device one letter at the time by changing the states using the control panel. Some of the letters are distorted because of the constraints of the fixed hexagonal pattern of the source/extractor array (see Figs. 2 and 3) and the blurring of some of the spray “spots” is due to the long exposure time of the camera.

We can selectively turn on an arbitrary number of ES sources, as long as the average flow rate is in the range of 0.2–0.6 cc/h/nozzle. The typical droplet size is 10 μm with the average flow rate of 0.4 cc/h at the stable cone-jet mode. Under the present conditions the shear rate is estimated at 10^4 s^{-1} , that is, one order of magnitude smaller as compared to IJP. Smaller droplets can be generated for different nozzle geometry. For a set flow rate, it is important to note that the droplet size (and therefore “spot size”) and flow rate/nozzle changes when there is a different number of nozzles “firing” since the total flow rate is partitioned equally among different number of nozzles. However, droplet diameter scales as $d_{\text{droplet}} \sim Q^\alpha$, where Q is the liquid flow rate and the exponent α is typically less than 0.5.¹² As a result, unless there are significant changes in the total number of fired sprays for the desired deposition pattern, this effect may be

modest. In a practical deposition tool, both the flow rate and deposition time may need to be modulated in real time to ensure constant spot size or volume dispensed.

B. System scale up

Multiple layers of flexible circuits are required in making the digital extractor because the trace wires that make electrical connection for the inner extractors have to come through the narrow gap between two neighboring extractors. The three-layer flexible circuit used for the prototype can be upgraded to eight layers, for which the electronic industry has well-developed fabrication processes. Such a circuit can easily accommodate ~ 600 sources with a design similar to the one shown in Fig. 3. Since we already demonstrated the operation of hundreds of sources with a microfabricated nozzle array,¹⁴ a digital ES system with $O(1000)$ sources is feasible with similar design. Of course, if the on/off control is applied to subgroups as opposed to individual extractors, systems with even greater number of sources can be realized.

C. Spatial resolution

For a stationary deposition device, the resolution of the deposition is determined by the distance between two neighboring nozzles. For this specific digital ES device discussed in this paper, the internozzle distance is 675 μm . We want to stress that the resolution of digital ES is not limited by the packing density of the nozzle array, which can have internozzle distance as small as 100 μm .¹⁴ The primary limiting factor is the possible arcing between two neighboring rings on the extractor as the scale is reduced. With careful insulation and high breakdown threshold environments such as CO_2 , it is realistic to achieve a pitch of 250 μm , which is comparable to the pitch of IJP nozzles and to the typical pixel size of liquid crystal display (LCD) monitors.

When the deposition device is mounted on a precision translational stage, which is the case for IJP print heads, the resolution is primarily determined by the droplet size. In this sense, the ES has a major advantage in resolution because it can generate much finer droplets as compared to IJP. In our multiplexed ESs, droplets with a diameter on the order of 1 μm are routinely generated in the stable cone-jet mode. As a comparison, the typical diameter of an IJP generated droplet is 50 μm . In terms of volume, the droplets from a digital ES are below 1 pl, which is two orders of magnitude smaller than those from a typical IJP, and can be as small as femtoliters. The presence of an electric charge on the droplet and the ensuing space charge may deteriorate the actual deposition resolution. But for a droplet travel distance on the order of 1 mm, a resolution comparable to the droplet diameter ought to be still achievable.

D. Response frequency

The highest switching frequency of the digital ES is limited by how fast the liquid meniscus responds to the sudden change in the external electric field. Marginean *et al.*¹⁶ used fast-lapse imaging to study the continuously pulsing mode of an ES. Here we focus on the phenomenology of the initiation of the cone-jet mode. With the aid of the high speed camera,

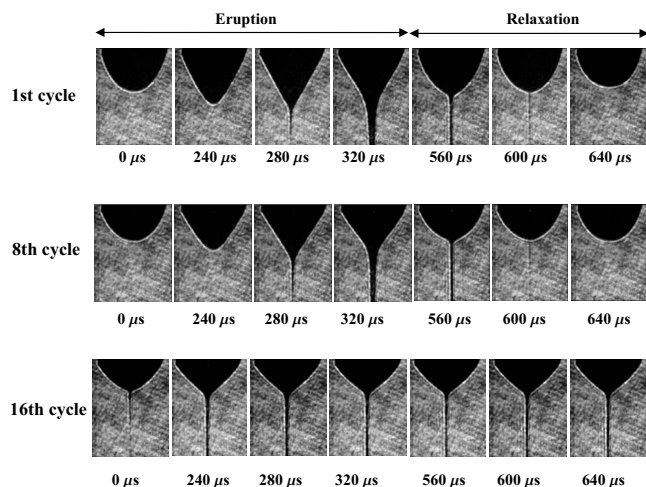


FIG. 7. Snapshots of three typical pulsing cycles of the transient process from hemispherical meniscus to cone-jet. Ethanol flow rate: 0.4 cc/h; camera speed: 25 000 fps.

we found that immediately after the high voltage was applied, the meniscus experienced several pulsing cycles before it converged to a stable cone-jet mode. Each cycle behaved very similarly. A few cycles are shown in Fig. 7. We can roughly distinguish two stages: eruption (0–320 μs) and relaxation (320–640 μs). In the eruption stage, the drop deforms from a hemisphere to a cone, and within 40 μs after the cone is formed (240–280 μs), a jet erupts from the cone tip. The jet diameter grows until approximately half way through the cycle (320 μs). In the relaxation stage (320–640 μs), the surface relaxes back to a hemisphere with a gradually thinner jet attached to the tip until the jet disappears and the next cycle starts. Each pulsing cycle lasts approximately 0.64 ms. Clearly, the droplets generated in the transient process do not retain the monodispersity of a stable cone-jet. After each cycle, the meniscus sheds more liquid than is fed, and the liquid meniscus volume gradually shrinks. Meanwhile, the two stages of eruption and relaxation become less distinguishable. At the 16th cycle, there is no longer a clear separation between the two stages and we can consider the meniscus has stably deformed to a steady cone-jet. The whole 16 cycles' transient process is highly repeatable and lasts 10 ms.

We shall now consider the necessary scaling of the response time of the process. Two variables are critically at play: surface tension λ and viscosity μ , with which we can formulate two characteristic times: the interfacial oscillation period $\tau_\lambda = \sqrt{\rho d^3 / \lambda}$ and the viscous damping time $\tau_\mu = \rho d^2 / \mu$. The ratio of these two times is the Ohnesorge number, Oh . Plugging in the values of the parameters in the experiment, i.e., $\rho = 789 \text{ kg/cm}^3$, $d = 210 \text{ }\mu\text{m}$, $\lambda = 0.0224 \text{ N/m}$, and $\mu = 0.0012 \text{ kg/(m s)}$, we obtain $\tau_\lambda = 0.57 \text{ ms}$ and $\tau_\mu = 29 \text{ ms}$, that are in satisfactory agreement with the measured ones of 0.64 and 10 ms, respectively. Rayleigh,¹⁷ in an inviscid analysis of the frequency of a freely oscillating drop with small vibration amplitudes, reported a characteristic frequency $f = \pi/4 \sqrt{\rho d^3 / \lambda}$, which is consistent with the presented scaling within a factor of order

unity. That frequency can also be derived by regarding the vibrating meniscus as an oscillator with oscillation frequency scaling as $f \propto \sqrt{m/k} \propto d^{-3/2}$, where m is the oscillator mass and k is a suitably defined spring constant that is independent of the mass.

In view of the disparity between the surface tension time and the viscous time, the meniscus is underdamped with $\text{Oh} \ll 1$ and will remain so even for a decrease in nozzle diameter by one order of magnitude, which is the most that is realizable in typical systems. We conclude that the response frequency is determined by τ_μ and decreases quickly as the nozzle outer diameter shrinks. For example, when d is decreased to 30 μm , $\tau_\mu \sim 0.6 \text{ ms}$, corresponding to a response frequency of O(kHz). For ethylene glycol, whose viscosity is 16 times higher than that of ethanol, the response frequency can reach O(10 kHz) for the same nozzle size.

IV. CONCLUSIONS

We demonstrated the concept of digital ES with a 61-source MES system, in which the individual ES source can be turned on and off independently and responsively. The nozzle array was microfabricated in silicon, and the individual nozzle control is achieved by changing the electric field near each nozzle with a digital extractor made of flexible circuits. This system showed a 100 Hz response frequency and 675 μm or better resolution. With similar design and fabrication procedures, it is feasible to reach O(1000) sources, 250 μm or better resolution, and a O(kHz) response frequency that is controlled by viscous damping time. This device has potential in many applications including controlled depositions of highly viscous substances and live liquid suspensions.

ACKNOWLEDGMENTS

We thank Mr. Edward Jackson from the Department of Electrical Engineering at Yale University for his help in designing the control panel and Mr. Eric Dube from Tech-Etch for his help in designing the digital extractor. The support of the U.S. Army under Cooperative Agreement No. W911NF-05-2-0015 is gratefully acknowledged.

- ¹B. R. Ringeisen, C. M. Othon, J. A. Barron, D. Young, and B. J. Spargo, *Biotechnology J.* **1**, 930 (2006).
- ²J. F. Dijkman, P. C. Duineveld, M. J. J. Hack, A. Pierik, J. Rensen, J.-E. Rubingh, I. Schram, and M. M. Vernhout, *J. Mater. Chem.* **17**, 511 (2007).
- ³B. Winther-Jensen and F. C. Krebs, *Sol. Energy Mater. Sol. Cells* **90**, 123 (2006).
- ⁴M. Mott and J. R. G. Evans, *Mater. Sci. Eng., A* **271**, 344 (1999).
- ⁵P. A. Meléndez, K. M. Kane, C. S. Ashvar, M. Albrecht, and P. A. Smith, *J. Pharm. Sci.* **97**, 2619 (2008).
- ⁶B.-J. de Gans, P. C. Duineveld, and U. S. Schubert, *Adv. Mater.* **16**, 203 (2004).
- ⁷T. Xu, J. Jin, C. Gregory, J. J. Hickman, and T. Boland, *Biomaterials* **26**, 93 (2005).
- ⁸M. Cloupeau and B. Prunet-Foch, *J. Electrostat.* **22**, 135 (1989).
- ⁹G. Taylor, *Proc. R. Soc. London, Ser. A* **280**, 383 (1964).
- ¹⁰J.-U. Park, M. Hardy, S. J. Kang, K. Barton, K. Adair, D. K. Mukhopadhyay, C. Y. Lee, M. S. Strano, A. G. Alleyne, J. G. Georgiadis, P. M. Ferreira, and J. A. Rogers, *Nature Mater.* **6**, 782 (2007).
- ¹¹D.-Y. Lee, Y.-S. Shin, S.-E. Park, T.-U. Yu, and J. Hwang, *Appl. Phys. Lett.* **90**, 081905 (2007).

- ¹²I. W. Lenggoro, H. M. Lee, and K. Okuyama, *J. Colloid Interface Sci.* **303**, 124 (2006).
- ¹³W. Deng and A. Gomez, *J. Aerosol Sci.* **38**, 1062 (2007).
- ¹⁴W. Deng, C. M. Waits, B. Morgan, and A. Gomez, *J. Aerosol Sci.* **40**, 907 (2009).
- ¹⁵W. Deng, J. F. Klemic, X. Li, M. A. Reed, and A. Gomez, *J. Aerosol Sci.* **37**, 696 (2006).
- ¹⁶I. Marginean, L. Parvin, L. Heffernan, and A. Vertes, *Anal. Chem.* **76**, 4202 (2004).
- ¹⁷L. Rayleigh, *Proc. R. Soc. London* **29**, 71 (1879).